HHS Public Access

Author manuscript

Nat Cell Biol. Author manuscript; available in PMC 2009 May 01.

Published in final edited form as:

Nat Cell Biol. 2008 November ; 10(11): 1257–1268. doi:10.1038/ncb1784.

Planar Polarization in Embryonic Epidermis Orchestrates Global Asymmetric Morphogenesis of Hair Follicles

Danelle Devenport[1] and **Elaine Fuchs**[1,*]

[1]Howard Hughes Medical Institute, Laboratory of Mammalian Cell Biology & Development, The Rockefeller University, New York, NY 10065

Abstract

Mammalian body hairs align along the anterior-posterior axis and offer a striking but poorly understood example of global cell polarization, a phenomenon known as planar cell polarity (PCP). We've discovered that during embryogenesis, dramatic changes in cell shape and cytoskeletal polarization occur as nascent hair follicles (HFs) become anteriorly angled, morphologically polarized and molecularly compartmentalized along the A–P axis. Interestingly, HF initiation coincides with asymmetric redistribution of Vangl2, Celsr1 and Fzd6 within the embryonic epidermal basal layer. Moreover, loss of function mutations in Vangl2 and Celsr1 unveil their essential role in HF polarization and orientation, which develop in part, through nonautonomous mechanisms. Vangl2 and Celsr1 are mutually required for their planar localization *in vivo*, and physically associate in a complex *in vitro*. Finally, we provide evidence *in vitro* that homotypic interactions of Celsr1 intercellularly are required to recruit Vangl2 and Fzd6 to sites of cell-cell contact.

Keywords

PCP; hair follicle; skin; planar; asymmetry; polarity; Vangl2; Celsr1; Fzd6

Introduction

PCP proteins transmit directional cues to align cells locally with their neighbours and globally with body axes1–3. PCP has been most extensively studied in *Drosophila*, where the first genes controlling this process were identified. *Frizzled* is the founding member of a group of core PCP components including *Strabismus*, *Flamingo* and *Dishevlled* that orient the polarity of hairs and bristles that cover the body surface and orient photoreceptor clusters in the fly eye2. Depending on the tissue, PCP orients either individual cells within an epithelial sheet or multicellular clusters, which polarize as a group. Core PCP components are functionally conserved in vertebrates3, and genetic mutations in mouse homologues of

*Correspondence should be addressed to E.E. (fuchslb@rockefeller.edu).

Author Contributions

D.D. designed, performed and analyzed the experiments and wrote the manuscript. E.F. supervised the project and wrote the manuscript.

Frizzled (*Fzd3, Fzd6*), *Strabismus* (*Vangl2*), *Flamingo* (*Celsr1*) and *Dishevelled* (*Dvl1, Dvl2*), result in embryonic failure of neural tube closure and misorientation of stereocilia bundles in the inner ear4–8.

The conservation of PCP genes suggests that PCP might have evolved to regulate similar morphogenetic processes in mammals. Like the fly wing, the mouse is covered with epidermal appendages that align along the anterior-posterior (A-P) axis of the body surface. However, in contrast to the wing where each cell emits a single hair, each mouse hair follicle (HF) is comprised of hundreds of proliferative cells that must orient as a unit in coordination with its neighbours, which are separated from one another by many intervening basal epidermal cells. Thus far, the only clue that a PCP pathway might control HF orientation comes from adult *Frizzled 6* null (*Fzd6−/−*) mice, which exhibit whorled hair patterns9, 10, similar to the wing hairs of *Drosophila Frizzled* mutants. However, *Frizzled* genes are known to affect canonical Wnt/β-catenin signalling as well as PCP11, and the underlying cellular and molecular basis for alterations in *Fzd6−/−* HFs is unknown. While no HF defects have been reported for the other PCP genes, this may have been overlooked due to embryonic lethality.

In this study, we've addressed how and when HFs become oriented in mouse skin and find that dramatic changes in actin organization, cell shape and gene expression accompany HF orientation during the earliest stages of HF morphogenesis. We firmly establish a role for PCP genes in global alignment of body hairs, and discover their requirement for polarized gene expression and cytoskeletal changes within individual follicles. We also find that, concomitant with HF initiation, polarization of PCP proteins occurs within the epidermal basal layer. Overall, we show that PCP within developing epidermis orchestrates polarized behaviours at the cellular and tissue-wide level. Our findings establish a foundation for future investigations into how complex multicellular structures are polarized along body axes.

Results

HF orientation is accompanied by polarized cell shape and cytoskeletal changes along the A–P axis

In mouse, HF morphogenesis is initiated at embryonic day E14.5 when placodes bud from epithelium in response to inductive signals from the underlying dermis. Further signals drive follicle downgrowth and progression from placode to germ to peg12, 13. E16.5 embryos contain HFs at these three developmental stages allowing us to determine when and how developing HFs acquire their orientation13.

We first addressed whether anterior orientation of HFs is driven by anterior-posterior differences in morphology or by differential growth rates14. Initially, as placode cells invaginated into underlying dermis they lacked A–P directionality (Fig. 1a,d,g,j). Shortly thereafter, cells residing at the apex of developing hair germs acquired distinct morphologies along the A–P axis. Cells on the anterior side constricted basally, while posterior cells adopted a columnar morphology (Fig. 1b).

As germs elongated, these shape differences were maintained and correlated with the acute anterior angle between epidermis and follicle (Fig. 1c). Observation of dorsal backskin along the planar axis revealed a striking polarization of developing HFs. Anterior cells expressed reduced E-cadherin and adopted an orientation distinct from those on the posterior side (Fig.1 e, f).

Asymmetric changes in both actin and keratin cytoskeletons accompanied HF polarization. As visualized in transgenic *K14-GFPactin* embryos,15 actin filaments were enriched in basal constrictions that formed anteriorly in polarized hair germs(Fig. 1h,i insets). In addition, keratin 5 (K5)-containing protrusions extended from basal epidermal cells towards hair germs only on their anterior side (Fig. 1k,l insets). Soon after HF downgrowth was initiated, cells displayed distinct cell shape and cytoskeletal morphologies depending on which side of HFs they resided.

To determine whether differential growth rates contributed to HF orientation, we pulsed E16.5 embryos for 1 hr with BrdU and quantified relative numbers of S-phase cells on anterior and posterior sides of developing HFs. No significant differences were observed in their rates of proliferation (Fig. 1m)16.

HFs exhibit polarized patterns of gene expression along the A–P axis

In addition to morphological asymmetry, gene expression was differentially regulated along the A–P axis of individual hair germs. P-Cadherin, ZO-1, and *Shh* mRNA were all upregulated anteriorly in the lower germ (Fig. 2a–b, e)17, while E-cadherin was downregulated (Fig 2c, arrowheads). NCAM, by contrast was upregulated posteriorly in the upper germ (Fig. 2d, arrows)18, 19. Notably, the appearance of asymmetric gene expression coincided with the first morphological signs of HF polarization (Fig. 1a–f; Supplementary Fig. S1).

The polarized patterns of gene expression along the A–P axis led us to wonder if cells within HFs might be physically compartmentalized. We used lineage tracing to determine the spatial relationship between anterior Shh-expressing hair germ cells and their descendents. Tamoxifen was used to irreversibly activate LacZ-expression in E15.5 *ShhCreER^{T2}/R26R* embryos20. Four days later (P0), LacZ-marked cells were found along the length of the centre and anterior but not posterior sides of HFs (Fig. 2f), suggesting that anterior *Shh*-expressing cells do not mix with posterior cells, and that developing HFs are compartmentalized along the A–P axis.

Vangl2 and Celsr1 are asymmetrically localized within the plane of interfollicular epidermis

Although *Fzd6* need not function exclusively in PCP, its role in patterning adult mouse HFs was suggestive that PCP might control HF orientation9. To investigate this possibility, we focused on Vangl2 and Celsr1, whose *Drosophila* homologues (Strabismus and Flamingo, respectively) are known to function in PCP, but not canonical Wnt signaling2.

Immunolabeling of Vangl2 and Celsr1 colocalized them to embryonic skin (Fig. 3a–b). Planar views through the base of hair germs revealed that the PCP cadherin Celsr1 was

asymmetrically distributed in individual germ cells along the A–P axis, while the adherens junction (AJ) E-cadherin was not (Fig. 3c-c' insets).

Vangl2 and Celsr1 were also expressed in interfollicular epithelium (IFE), where they were restricted to the lateral sides of basal epidermal cells (Fig. 3d–e). Compared to E-cadherin, which was distributed uniformly at cell-cell borders (Fig. 3f',g'), Vangl2 and Celsr1 were enriched along the A–P axis (Fig. 3f,g). This pattern was reminiscent of PCP distribution in the *Drosophila* wing 21–23 and mouse inner ear7, 8, 24 but unlike these tissues, mouse epidermal basal cells do not exhibit obvious morphological signs of planar polarity. Instead, planar polarization within the basal layer more closely resembled epithelia that surround and give rise to *Drosophila* ommatidia25, 26 or sensory bristles27 which, like HFs, are examples of polarized multicellular units.

Asymmetric localization of PCP proteins occurs early and requires directional cues for establishment but not maintenance

The polarization within the embryonic basal layer provided a potential explanation for how HFs, derived from basal cells, might acquire A–P directional information and collectively polarize. Interestingly at E12.5, Celsr1 was uniformly distributed at cell-cell borders of the single-layered skin epithelium (Fig. 4a). At the onset of stratification (~E13.5), Celsr1 distribution was enriched along the A–P axis (Fig. 4b). By E14.5, Celsr1 was polarized on A–P sides of basal cell membranes (Fig. 4c). This timing coincided with the earliest signs of HF morphogenesis.

To determine whether establishment and maintenance of PCP requires directional cues from the embryo, we cultured backskin explants from embryos at E13.5 after epidermal PCP had initiated, and E14.5 after epidermal PCP was established. Interestingly, within 2d of *ex vivo* growth, E13.5 cultured skins lacked A–P polarity: Celsr1 became unpolarized within the basal epidermal layer (Fig. 4d), and HFs grew straight downward (Fig. 4d').

In contrast, 2d E14.5 skin cultures maintained epidermal polarization of Celsr1, and generated HFs that oriented towards what was the embryonic anterior (Fig. 4e, e'). Moreover, by 3d, the second wave of hair germs initiated and aligned with neighbouring, more mature follicles (not shown). These collective findings suggest that a directional signal acquired between E13.5-E14.5 is necessary to maintain asymmetric PCP distribution and generate A–P polarization in developing HFs.

Interestingly, once epidermal PCP was fully established *in vivo*, it was maintained *in vitro*. However *in vivo*, when skins from embryos E17.5 or younger were rotated 180 degrees and grafted onto adult hosts, HFs across the graft reoriented anteriorly towards the host body axis (Supplementary Fig. S2). Thus once established, PCP can continue to respond to directional cues.

PCP proteins localize asymmetrically independently of epidermal stratification or HF morphogenesis

Since temporal redistribution of PCP proteins coincided with HF morphogenesis and epidermal stratification/differentiation, we wondered whether PCP polarization might

depend upon these morphogenetic events. To test this, we examined *Shh* null embryos, where hair placodes specify but fail to elongate28, and conditional epithelial *β-catenin* null embryos, where placodes fail to form29. In both mutants, Celsr1 was properly expressed and in basal epidermal cells and polarized along the A–P axis (Fig. 4f–i). Celsr1 asymmetry also developed normally in *p63*-null epidermal cells, even though loss of p63 blocks both stratification and HF induction30, 31(Fig. 4j–k). Thus, PCP within the basal layer develops early and independently of events necessary for stratification, placode specification and HF downgrowth.

Vangl2 and Celsr1 are necessary for orientating HFs along the A–P axis

To determine whether PCP is required for HF patterning, we utilized mouse mutants *Looptail (Lp)* and *Crash (Crsh)*, which harbour point mutations in *Vangl2* and *Celsr1* genes, respectively4, 5. Although these homozygous mutant embryos display neural tube and inner ear defects, many survive until E18.5. At this age, *Lp/Lp* and *Crsh/Crsh* embryos displayed HFs that were misangled compared to heterozygous littermates (Fig. 5, a–c). Measuring counter clockwise, WT follicles pointed anteriorly with an average acute angle of 55° (n=112) (Fig. 5e). By contrast, most *Lp/Lp* and *Crsh/Crsh* HFs pointed straight downward with an average angle of 88° (n=109) and 92° (n=132), respectively. As HFs developed they became randomly oriented, as visualized by whole mount imaging of E18.5 *Lp/Lp* backskins expressing GFP-actin (Fig. 5f–g).

The HF phenotype in *Lp/Lp* and *Crsh/Crsh* embryos was specific, as we did not detect significant defects in HF density, epidermal stratification, differentiation or integrity (Fig. 5a–c; Supplementary Fig. S3). Moreover, HF misorientation was not a secondary consequence of an open neural tube (where skin fails to cover the dorsal midline) because another mutant, *Circletail* (*Crc/Crc*), displayed neural tube defects6, 32 but exhibited properly aligned HFs (Fig. 5d, e).

Vangl2 and Celsr1 are necessary for A–P polarization of cell shape, cytoskeletal organization and gene expression within HFs

The orientation defect in *Lp* and *Crsh* mutant follicles suggested that individual HFs might have lost A–P polarization. Indeed several polarized features were lost in *Lp/Lp* and *Crsh/Crsh* mutant hair germs: 1) anterior germ cells adjacent to epidermis failed to constrict basally (Fig. 6a–b; Fig. S4a); 2) viewed dorsally, mutant germs appeared circular (Fig. 6c–d; Fig. S4b); 3) GFPactin failed to accumulate basally in anterior germ cells, while gaps in cortical actin formed in central germ cells (Fig. 6e–f); 4) basal keratin protrusions, normally found anteriorly, were found on both sides of mutant follicles (Fig. 6g–h; Fig. S4c).

Polarized gene expression patterns were also lost in *Lp/Lp* and *Crsh/Crsh* hair germs. Cells expressing *Shh*, P-cadherin and ZO-1, but reduced E-cadherin were distributed uniformly throughout the base of mutant germs rather than anteriorly (Fig. 6i–n; Fig. S4d–e; data not shown). Analogously, NCAM was expressed symmetrically rather than posteriorly (Fig. 6o–p; FigS4f). These data exposed a role for Vangl2 and Celsr1 not only in global alignment of HFs, but also in polarization of individual follicles.

Nonautonomous functions for Vangl2 in HF polarization

PCP is thought to propagate from cell to cell through communication between neighbouring cells1, 33. In *Drosophila* wings, clones of cells mutant for Strabismus disrupt the polarity of adjacent WT cells34, 35. To determine whether mouse Vangl2 can similarly function nonautonomously in skin, we generated chimeric WT and *Lp/Lp* mouse embryos (see Materials and Methods). Strikingly, WT HFs that were surrounded by *Lp/Lp* mutant epidermal cells invariably failed to polarize. Such follicles were not only misoriented, but they also failed to express NCAM, P-Cadherin and E-Cadherin in a polarized pattern (Fig. 6q; and data not shown). Thus, both morphological and molecular polarizations of HFs require nonautonomous functions of Vangl2.

Vangl2 and Celsr1 are interdependent for their polarized distribution in the basal layer

Vangl2 and Celsr1 have been genetically implicated in PCP, but their functional relationship remains poorly understood. *Lp* harbours an S464N mutation in Vangl2's C-terminal cytoplasmic domain4, resulting in dramatically reduced Vangl2 at skin cell borders (Fig. 7a–b). Despite the reduction of Vangl2 in *Lp/Lp* epidermis, Celsr1 still localized to cell borders. However, rather than distributing asymmetrically as in WT, Celsr1 was distributed uniformly at membrane junctions (Fig. 7d–e)21.

Celsr1 encodes an atypical cadherin and the *Crsh* allele harbours a D1040G mutation within its extracellular domain5 that eliminated Celsr1's asymmetric localization without affecting its overall expression or transport to the plasma membrane (Fig. 7f). Vangl2 protein, however, not only failed to polarize in *Crsh/Crsh* epidermis, but also appeared punctate at many intercellular borders, possibly reflective of defective delivery/stabilization at cell-cell borders (Fig. 7c)21, 36. These findings indicate a dependency of Vangl2 and Celsr1 on one another for their proper asymmetric distribution along the A–P axis.

To dissect the mechanisms that localize PCP proteins, we examined Celsr1^{WT}GFP in primary epidermal keratinocytes *in vitro*, where Celsr1 is not normally expressed. In isolated transfected keratinocytes within an epithelial sheet, Celsr1^{WT}GFP was diffuse (Fig. 7g). By contrast, wherever two transfected cells were neighbours within the sheet, Celsr1^{WT}GFP localized sharply and exclusively to the contacting interface (Fig. 7h). Thus, Celsr1 seemed to form homotypic intercellular interactions22, 37 required for its membrane stabilization.

Interestingly, Celsr1 homotypic interactions were dependent on calcium (Fig. 7i), but this was not due to a dependence upon adherens junction formation, since Celsr1 still localized to contacting interfaces in calcium-treated α-*catenin*-null cells38 (Fig. 7j). Celsr1GFP localization to contacting interfaces was strongly impaired by the extracellular *Crsh* mutation (Fig. 7k) and partially impaired by deletion of the cytoplasmic tail (Fig. 7l).

As we observed *in vivo*, Vangl2's behavior *in vitro* was very different from that of Celsr1 (Fig. 7m–p). Even when two adjacent cells expressed Vangl2-Cherry, the protein remained cytoplasmic (Fig. 7n). Cotransfection of Celsr1^{WT}GFP was sufficient to recruit Cherry-Vangl2 to the contacting interface between cotransfected cells (Fig. 7p). By contrast, Vangl2-Cherry only weakly localized to cell contacts in Celsr1^{Crsh}GFP- or Celsr1$^{\Delta cyto}$GFP-expressing keratinocytes (Fig. 7q,r). Interestingly, the amount of Vangl2-Cherry localized to

the membrane appeared to be roughly proportional to the level of mutant Celsr1 at cell contacts, suggesting the *Crsh* and $^{\Delta cyto}$ mutations primarily disrupted Celsr1's homotypic interaction, and not its ability to recruit Vangl2. By contrast, deletion of Vangl2's entire C-terminal cytoplasmic tail or introduction of the *Lp* point mutation (S464N) within it resulted in a failure of Vangl2 to be recruited by Celsr1 (Fig. 7s–t). The overall Vangl2^{Lp} surface levels were comparable to WT, indicating that transport to the plasma membrane is not the primary defect caused by the Lp mutation (Fig. 7u). Rather, since Flag-Vangl2^{WT} but not Flag-Vang^{Lp} coimmunoprecipitated with Celsr1^{WT}-Myc (Fig. 7v), it's possible that the phenotypic defects caused by *Lp* mutation are rooted in its inability to physically associate with Celsr1. These findings reinforced those *in vivo*, and suggested that Vangl2 is dependent upon Celsr1 not only for its planar distribution but also for efficient localization/stabilization at cell-cell borders21, 37.

Frizzled-6 is asymmetrically localized in epidermis and is recruited to cell contacts by Celsr1

The misalignment of HFs described in adult *Fzd6* null mice suggested a role for Fzd6 in a PCP-like pathway in skin development9. Indeed, Fzd6 was expressed in embryonic skin in a pattern indistinguishable from Vangl2 and Celsr1 (Fig. 8a–c). Additionally, in the absence of functional Celsr1 or Vangl2, Fzd6 protein adopted a more uniform distribution, revealing a dependency upon both Celsr1 and Vangl2 (Fig. 8d–e)21, 23, 26.

To further explore the interaction between these three proteins, we expressed Fzd6-Cherry in keratinocyte monolayers, where it showed a perinuclear-enriched cytoplasmic distribution similar to Vangl2-Cherry (Fig. 8f). On its own Fzd6-Cherry remained cytoplasmic, even when two expressing cells came into direct contact (shown). Cotransfection with Celsr1-GFP was sufficient to recruit Fzd6-Cherry to cell borders, but only to the contacting surface between two Celsr1-expressing cells (Fig. 8g). In contrast to its asymmetric localization (Fig. 8d), Fzd6's recruitment to cell borders was not dependent on WT Vangl2, as Celsr1 still localized Fzd6-Cherry in *Lp/Lp* keratinocytes (Fig. 8h).

The dependence of Fzd6 on Celsr1 was not limited to overexpressed Fzd6-Cherry protein, as endogenous Fzd6, which was diffusely distributed in keratinocytes lacking Celsr1-GFP, shifted its localization to cell borders in a homotypic Celsr1-dependent manner (Fig. 8i)37. Together with genetic data demonstrating a requirement for *Fzd6* in adult HF orientation, our results strongly suggest that a conserved PCP pathway operates early in mammalian epidermis to coordinately polarize HFs across body axes.

Discussion

In this study we have addressed how global polarization of HFs is established across the anterior-posterior axis during embryonic skin development. Our data demonstrate that in skin, conserved PCP genes control polarized behaviours at cellular, appendage, and tissue levels. Early in embryogenesis, PCP proteins act to polarize basal epidermal cells though their asymmetric distribution along the planar axis. The fact that this occurs independently of β-catenin, Shh and p63 indicates that the signals controlling planar polarization are among the earliest developmental cues known to govern epidermal and HF morphogenesis12.

Given the role for Fzd6 in patterning adult HFs8, 9 and our findings implicating Fzd6 in a common pathway with Celsr1 and Vangl2, the ligands for Fzd receptors i.e. Wnt-secreted morphogens, seem likely candidates for the graded spatial signals that establish PCP in embryonic epidermis. While Wnts are dispensable for PCP in *Drosophila*37, 39, Wnt11 is required for convergent extension in vertebrates 40, 41. Moreover, *Wnt5a* null mice display mild PCP inner ear defects and genetically interacts with Vangl242. Although it remains unknown whether any of these Wnts provide graded instructional cues for directionality, skin expresses many different Wnts at the right place and time to have an impact on PCP43.

Whatever the nature of this early signal that establishes PCP, its sustained activity through E13.5 appears to be essential, as only organ cultures of E14.5 maintained asymmetric distribution of PCP proteins *in vitro*. Of additional interest is how PCP proteins become redistributed within the membrane in response to this cue. The finding that Celsr1 forms calcium-dependent intercellular interactions necessary to recruit Vangl2 and Fzd6 suggest that Celsr1 homodimers lie at the top of a hierarchy for PCP protein localization21. Our studies with Crsh suggest that Celsr1's extracellular interactions are important for redistributing PCP proteins. These findings are consistent with a recent *Drosophila* study demonstrating a critical role for Flamingo homodimers in recruiting Strabismus and Frizzled to opposing cell contacts 37.

Once PCP is established within the epidermal plane, it's important in specifying subsequent polarized behaviours on the A–P sides of hair placodes. We've uncovered dramatic A–P differences in cytoskeleton and gene expression which fail when PCP is compromised. The precise mechanisms responsible for these downstream polarized behaviours are still unclear. However, the morphological polarization within HFs could be controlled by mechanisms similar to fly wing, where a PCP pathway acts through Rho-kinase and myosin to regulate the actin cytoskeleton in individual epidermal cells44. Additionally, PCP could directly influence polarized gene expression in HFs by biasing the direction of one or more downstream signalling pathways. In this regard, it could be relevant that in *Drosophila* eye, Frizzled acts to bias directionality of Notch signaling45–48, which has also been implicated in A–P patterning of feather buds49.

In summary, our findings shed light on how multicellular units spatially separated from one another can become coordinately and globally polarized. We propose that HFs acquire directional information through basal epidermal cells, which become polarized along the A–P axis concurrent with HF induction. By setting up A–P directionality in cells from which HFs derive, and maintaining it through successive waves of HF induction, directional information can be translated, continuously, to emerging HFs.

Materials and Methods

Mouse lines and Breeding

*K14-GFPactin*15, *K14-H2BGFP*50 mice have been described. *Looptail* mutant mice (LPT/Le stock, Jackson Laboratories) were provided by M.W. Kelley. *Crash mutant* mice5 were from J. Murdoch; *Circletail*32 mice were from R. Rachel. For Shh lineage tracing, *ShhCreER*^{T2}/+ mice20 were crossed to *ROSA26*$^{Flox\text{-}Stop\text{-}Flox\text{-}\beta geo}$ (*R26R)* animals. To

generate *Lp/Lp* embryos that express GFP-actin, we established *Lp/+; K14-GFPactin/+* lines and mated together double heterozygous mice.

ShhCreER induction and X-Gal staining

Pregnant *ShhCreERt2/+; R26R/+* females carrying E15.5 embryos were injected with 5mg Tamoxifen in corn oil. Cryosections from newborn backskins were fixed 2 minutes in 0.5% glutaraldehyde in PBS and stained overnight 37°C in X-Gal staining solution (100mM $NaPO_4$ pH 7.3, 1.3 mM $MgCl_2$, 3mM $K_3Fe(CN)_6$, 3mM $K_4Fe(CN)_6$, 1mg/ml X-Gal). Sections were counterstained with anti-K5 primary antibodies and anti-rabbit-HRP secondaries (Jackson Laboratories). DAB (3,3'-diaminobenzidine) staining was used for immunodetection (DakoCytomation).

Quantification of HF angles

OCT sections from ≥4 *Lp/Lp*, *Crsh/Crsh* and *Crc/Crc* E18.5 embryos and WT littermates were fixed and stained with K5 antibodies. Low magnification (10x) images HFs across backskin were captured using an Axioplan microscope (Carl Zeiss MicroImaging) equipped with an Orca-ER camera (Hamamatsu). Angles between IFE and HF on the anterior side were calculated using ImageJ software angle tool. Angle data was plotted using OriginLab 7.5 software.

Generation of Celsr1 antibody

A 303 bp fragment (a.s. 2885–2985) of Celsr1 was cloned into BamH1 and EcoR1 sites of pGEX4T-1. Guinea pigs were immunized with the 101 a.a. Celsr1 fragment fused to GST. Antiserum was affinity-purified against the GST-fusion protein.

Embryo preparation and Immunofluorescence

For immunofluorescence on sagittal sections, embryos were embedded in OCT, frozen, cryosectioned (10–30um) and fixed 10 minutes in 4% formaldehyde in PBS. Sections were permeablized 10 minutes in PBS+0.1%Triton (PBST) and blocked 1 hour in 2.5% fish gelatin, 2.5% normal donkey serum, 2.5% normal goat serum, 0.5% BSA, 0.1% Triton, 1X PBS. Primary antibodies were incubated for either 2 hours r.t. or overnight at 4°C at the following dilutions: E- and P-Cadherin (rat, 1:100, M. Takeichi, RIKEN, Kobe), K5 (rabbit, 1:1000, Fuchs Lab), ZO-1 (rabbit, 1:200, Zymed), NCAM (rat, 1:200, Chemicon), Vangl224 (rabbit, 1:500, M. Montcouquiol), Celsr1 (guinea pig, 1:200, D.D. Fuchs Lab), Fzd6 (goat, 1:400, R&D Sysytems). Secondary antibodies coupled to Alexa Fluor 488 (Invitrogen), Rhodamine Red X and Cy5 (Jackson Laboratories) were diluted 1:400 and incubated 2hrs at r.t. For whole mount immunofluorescence, embryos were fixed 1hr in 4% formaldehyde. Backskins were dissected and processed for immunofluorescence as above except that 0.3% Triton was substituted for 0.1% Triton and all antibody incubations were performed overnight at 4°C.

Confocal microscopy and image processing

Images were acquired with a Zeiss LSM510 laser-scanning microscope (Carl Zeiss MicroImaging) through a 63x oil objective (N.A. 1.4) For whole mount imaging, Z-stacks of

15–40 planes (0.5μm) were captured. Representative single Z-planes are presented. Images were recorded at 1024×1024 square pixels representing a 146μm×146μm area. K14-GFPactin E18.5 whole mount images were collected through a 10x objective (N.A. 0.8) and Z-stacks of 15–20 planes (2.5μm) were captured. Z-stacks were projected using ImageJ software. RGB images were assembled in Adobe Photoshop CS2 v. 9.0.2 and panels were labelled in Adobe Illustrator CS2 v. 12.0.1.

BrdU pulse-chase and quantification

Pregnant CD1 females carrying E16.5 embryos were injected with 50μg/g body weight Bromo-2'-deoxyuridine (BrdU) and embryos were harvested after 1hr. Frozen sections (10μm) were fixed in 4% PFA in PBS, washed and incubated in 1N HCl for 1hr at 37°C prior to staining with BrdU (rat, 1:400, AbCam) and K5 antibodies. BrdU-positive cells within placodes and hair germs from four different embryos were counted and classified as either anterior or posterior based on their position relative to the central portion of the HF.

Skin culture

Backskins were dissected from E13.5 and E14.5 *K14-GFPactin* embryos in cold, sterile PBS. Skins were placed dermis-side down onto Whatman Nucleopore TrackEtch filters (Spi Supplies) and allowed to attach for 10 minutes. Filters were placed in 12-well plates and floated on pre-warmed keratinocyte culture medium with 0.3 mM calcium. After culturing 2–3d at 37°C, 7.5% CO_2, skins were fixed and processed for immunofluorescence.

Cloning of Celsr1, Vangl2, and Fzd6 constructs

Full-length Celsr1, Vangl2, and Fzd6 cDNAs were cloned by RT-PCR from E18.5 mouse epidermal RNA and subcloned into pCR2.1-TOPO. Clones were verified by sequencing. For C-terminal tagging, Celsr1 was cloned in frame into Bgl2 and HindIII sites of pEGFPN1 (for EGFP tagging; Clontech) or BamH1 and HindIII sites of pCMV3Tag-9 (for 3xMyc tagging; Stratagene). The *Crsh* mutation (D1040G) was introduced by site directed mutagenesis into a Sal1-Sph1 fragment of Celsr1 and then subcloned into the full-length construct. To generate N-terminally tagged Cherry-Vangl2, a Spe1-mCherry-Bgl2 fragment was ligated in frame to Bgl2-Vangl2-Sal1 and K14-β-globin-MCS vector (Fuchs lab). The *Lp* mutation (S464N) was introduced by site-directed mutagenesis. pCMV3Tag-1a (Stratagene) was used for N-terminally Flag tagged Vangl2 constructs. For Fzd6-Cherry, Bgl2-Fzd6-EcoR1 and EcoR1-mCherry-Sal1 were ligated to BamH1 and Xho1-digested K14-β-globin-MCS.

Cell culture

Mouse keratinocytes were cultured and maintained in E-media supplemented with 15% serum and 0.05mM Ca^{2+}. For Celsr1GFP, Cherry-Vangl2 and Fzd6-Cherry transfection experiments, keratinocytes were plated onto fibronectin-coated coverslips in 12-well dishes (70,000 cells/well). 12–24hrs after plating, cells were transfected with 800ng DNA using FuGENE transfection reagent (Roche). 24hrs after transfection, cells were shifted to high Ca^{2+} (>1mM) E-media for 12 or 24hrs after which cells were fixed and processed for immunofluorescence.

Surface Biotinylation and Coimmunoprecipitation

48hrs after transfection with Flag-Vangl2^{WT}or Flag-Vangl2^{Lp}, surface proteins were labelled with biotin for 30', then extracted 45' on ice, (Cadherin extraction buffer: 50 mM Tris pH7.4, 150mM NaCl, 5mM $CaCl_2$, 5mM $MgCl_2$, 1%NP-40, 1%TritonX) and recovered with streptavidin-coated sepharose beads (Pierce). For coimmunoprecipitation, extracts from keratinocytes transfected with Celsr1-Myc and/or Flag-Vangl2^{WT} and Flag-Vangl2^{Lp} and grown in high Ca^{2+} medium were immunoprecipitated with anti-c-Myc Abs (4 μg; Stratagene).

Generation of *Lp* Chimeras

Chimeric mice were generated by aggregating WT and *Lp/Lp* embryos at the 8-cell stage after removal of their zona pelucida. Aggregates were allowed to develop into blastocysts ex vivo, and after 24hrs were transferred to pseudo-pregnant females. Chimeric embryos were harvested at E16.5. WT cells were distinguished from homozygous *Lp* mutant cells by Vangl2 antibody staining.

Supplementary Material

Refer to Web version on PubMed Central for supplementary material.

Acknowledgements

We thank J. Murdoch, K. Anderson, M. Kelley, R. Rachel, B. Lake, and C. Tabin, for mice and embryos; M. Montcouquiol, S. Sokol, and M. Takeiechi for antibodies and reagents; L. Polak, N. Stokes, and LARC staff for care and breeding of mice; J. Zallen, S. Sokol, A. vandenBerg for helpful discussions; Alison North and Rockefeller's Bioimaging Resource Centre for assistance with image acquisition and analysis; J. Racelis and A. Firland-Schill for experimental assistance; and B. Short, V. Horsley, and J. Nowak for advice and critical reading of the manuscript. D.D. is a Ruth L. Kirschstein NRSA Postdoctoral Fellow. This work was supported by a grant from the National Institutes of Health (R01 AR27883). E.F. is an Investigator of the Howard Hughes Medical Institute.

References

1. Zallen JA. Planar polarity and tissue morphogenesis. Cell. 2007; 129:1051–1063. [PubMed: 17574020]
2. Seifert JR, Mlodzik M. Frizzled/PCP signalling: a conserved mechanism regulating cell polarity and directed motility. Nat Rev Genet. 2007; 8:126–138. [PubMed: 17230199]
3. Jones C, Chen P. Planar cell polarity signaling in vertebrates. Bioessays. 2007; 29:120–132. [PubMed: 17226800]
4. Kibar Z, et al. Ltap, a mammalian homolog of Drosophila Strabismus/Van Gogh, is altered in the mouse neural tube mutant Loop-tail. Nat Genet. 2001; 28:251–255. [PubMed: 11431695]
5. Curtin JA, et al. Mutation of Celsr1 disrupts planar polarity of inner ear hair cells and causes severe neural tube defects in the mouse. Curr Biol. 2003; 13:1129–1133. [PubMed: 12842012]
6. Montcouquiol M, et al. Identification of Vangl2 and Scrb1 as planar polarity genes in mammals. Nature. 2003; 423:173–177. [PubMed: 12724779]
7. Wang J, et al. Dishevelled genes mediate a conserved mammalian PCP pathway to regulate convergent extension during neurulation. Development. 2006; 133:1767–1778. [PubMed: 16571627]
8. Wang Y, Guo N, Nathans J. The role of Frizzled3 and Frizzled6 in neural tube closure and in the planar polarity of inner-ear sensory hair cells. J Neurosci. 2006; 26:2147–2156. [PubMed: 16495441]

9. Guo N, Hawkins C, Nathans J. Frizzled6 controls hair patterning in mice. Proc Natl Acad Sci U S A. 2004; 101:9277–9281. [PubMed: 15169958]
10. Wang Y, Badea T, Nathans J. Order from disorder: Self-organization in mammalian hair patterning. Proc Natl Acad Sci U S A. 2006; 103:19800–19805. [PubMed: 17172440]
11. Axelrod JD, McNeill H. Coupling planar cell polarity signaling to morphogenesis. ScientificWorldJournal. 2002; 2:434–454. [PubMed: 12806028]
12. Fuchs E. Scratching the surface of skin development. Nature. 2007; 445:834–842. [PubMed: 17314969]
13. Schmidt-Ullrich R, Paus R. Molecular principles of hair follicle induction and morphogenesis. Bioessays. 2005; 27:247–261. [PubMed: 15714560]
14. Chodankar R, et al. Shift of localized growth zones contributes to skin appendage morphogenesis: role of the Wnt/beta-catenin pathway. J Invest Dermatol. 2003; 120:20–26. [PubMed: 12535194]
15. Vaezi A, Bauer C, Vasioukhin V, Fuchs E. Actin cable dynamics and Rho/Rock orchestrate a polarized cytoskeletal architecture in the early steps of assembling a stratified epithelium. Dev Cell. 2002; 3:367–381. [PubMed: 12361600]
16. Magerl M, et al. Patterns of proliferation and apoptosis during murine hair follicle morphogenesis. J Invest Dermatol. 2001; 116:947–955. [PubMed: 11407986]
17. Bitgood MJ, McMahon AP. Hedgehog and Bmp genes are coexpressed at many diverse sites of cell-cell interaction in the mouse embryo. Dev Biol. 1995; 172:126–138. [PubMed: 7589793]
18. Hardy MH, Vielkind U. Changing patterns of cell adhesion molecules during mouse pelage hair follicle development. 1. Follicle morphogenesis in wild-type mice. Acta Anat (Basel). 1996; 157:169–182. [PubMed: 9226036]
19. Muller-Rover S, Peters EJ, Botchkarev VA, Panteleyev A, Paus R. Distinct patterns of NCAM expression are associated with defined stages of murine hair follicle morphogenesis and regression. J Histochem Cytochem. 1998; 46:1401–1410. [PubMed: 9815282]
20. Harfe BD, et al. Evidence for an expansion-based temporal Shh gradient in specifying vertebrate digit identities. Cell. 2004; 118:517–528. [PubMed: 15315763]
21. Bastock R, Strutt H, Strutt D. Strabismus is asymmetrically localised and binds to Prickle and Dishevelled during Drosophila planar polarity patterning. Development. 2003; 130:3007–3014. [PubMed: 12756182]
22. Usui T, et al. Flamingo, a seven-pass transmembrane cadherin, regulates planar cell polarity under the control of Frizzled. Cell. 1999; 98:585–595. [PubMed: 10490098]
23. Strutt DI. Asymmetric localization of frizzled and the establishment of cell polarity in the Drosophila wing. Mol Cell. 2001; 7:367–375. [PubMed: 11239465]
24. Montcouquiol M, et al. Asymmetric localization of Vangl2 and Fz3 indicate novel mechanisms for planar cell polarity in mammals. J Neurosci. 2006; 26:5265–5275. [PubMed: 16687519]
25. Das G, Reynolds-Kenneally J, Mlodzik M. The atypical cadherin Flamingo links Frizzled and Notch signaling in planar polarity establishment in the Drosophila eye. Dev Cell. 2002; 2:655–666. [PubMed: 12015972]
26. Strutt D, Johnson R, Cooper K, Bray S. Asymmetric localization of frizzled and the determination of notch-dependent cell fate in the Drosophila eye. Curr Biol. 2002; 12:813–824. [PubMed: 12015117]
27. Bellaiche Y, Beaudoin-Massiani O, Stuttem I, Schweisguth F. The planar cell polarity protein Strabismus promotes Pins anterior localization during asymmetric division of sensory organ precursor cells in Drosophila. Development. 2004; 131:469–478. [PubMed: 14701683]
28. St-Jacques B, et al. Sonic hedgehog signaling is essential for hair development. Curr Biol. 1998; 8:1058–1068. [PubMed: 9768360]
29. Huelsken J, Vogel R, Erdmann B, Cotsarelis G, Birchmeier W. beta-Catenin controls hair follicle morphogenesis and stem cell differentiation in the skin. Cell. 2001; 105:533–545. [PubMed: 11371349]
30. Yang A, et al. p63 is essential for regenerative proliferation in limb, craniofacial and epithelial development. Nature. 1999; 398:714–718. [PubMed: 10227294]

31. Mills AA, et al. p63 is a p53 homologue required for limb and epidermal morphogenesis. Nature. 1999; 398:708–713. [PubMed: 10227293]
32. Murdoch JN, et al. Circletail, a new mouse mutant with severe neural tube defects: chromosomal localization and interaction with the loop-tail mutation. Genomics. 2001; 78:55–63. [PubMed: 11707073]
33. Lawrence PA, Struhl G, Casal J. Planar cell polarity: one or two pathways? Nat Rev Genet. 2007; 8:555–563. [PubMed: 17563758]
34. Taylor J, Abramova N, Charlton J, Adler PN. Van Gogh: a new Drosophila tissue polarity gene. Genetics. 1998; 150:199–210. [PubMed: 9725839]
35. Adler PN, Taylor J, Charlton J. The domineering non-autonomy of frizzled and van Gogh clones in the Drosophila wing is a consequence of a disruption in local signaling. Mech Dev. 2000; 96:197–207. [PubMed: 10960784]
36. Das G, Jenny A, Klein TJ, Eaton S, Mlodzik M. Diego interacts with Prickle and Strabismus/Van Gogh to localize planar cell polarity complexes. Development. 2004; 131:4467–4476. [PubMed: 15306567]
37. Chen WS, et al. Asymmetric homotypic interactions of the atypical cadherin flamingo mediate intercellular polarity signaling. Cell. 2008; 133:1093–1105. [PubMed: 18555784]
38. Vasioukhin V, Bauer C, Yin M, Fuchs E. Directed actin polymerization is the driving force for epithelial cell-cell adhesion. Cell. 2000; 100:209–219. [PubMed: 10660044]
39. Lawrence PA, Casal J, Struhl G. Towards a model of the organisation of planar polarity and pattern in the Drosophila abdomen. Development. 2002; 129:2749–2760. [PubMed: 12015301]
40. Heisenberg CP, et al. Silberblick/Wnt11 mediates convergent extension movements during zebrafish gastrulation. Nature. 2000; 405:76–81. [PubMed: 10811221]
41. Tada M, Smith JC. Xwnt11 is a target of Xenopus Brachyury: regulation of gastrulation movements via Dishevelled, but not through the canonical Wnt pathway. Development. 2000; 127:2227–2238. [PubMed: 10769246]
42. Qian D, et al. Wnt5a functions in planar cell polarity regulation in mice. Dev Biol. 2007; 306:121–133. [PubMed: 17433286]
43. Reddy S, et al. Characterization of Wnt gene expression in developing and postnatal hair follicles and identification of Wnt5a as a target of Sonic hedgehog in hair follicle morphogenesis. Mech Dev. 2001; 107:69–82. [PubMed: 11520664]
44. Winter CG, et al. Drosophila Rho-associated kinase (Drok) links Frizzled-mediated planar cell polarity signaling to the actin cytoskeleton. Cell. 2001; 105:81–91. [PubMed: 11301004]
45. Gho M, Schweisguth F. Frizzled signalling controls orientation of asymmetric sense organ precursor cell divisions in Drosophila. Nature. 1998; 393:178–181. [PubMed: 9603522]
46. Cooper MT, Bray SJ. Frizzled regulation of Notch signalling polarizes cell fate in the Drosophila eye. Nature. 1999; 397:526–530. [PubMed: 10028969]
47. Tomlinson A, Struhl G. Decoding vectorial information from a gradient: sequential roles of the receptors Frizzled and Notch in establishing planar polarity in the Drosophila eye. Development. 1999; 126:5725–5738. [PubMed: 10572048]
48. Fanto M, Mlodzik M. Asymmetric Notch activation specifies photoreceptors R3 and R4 and planar polarity in the Drosophila eye. Nature. 1999; 397:523–526. [PubMed: 10028968]
49. Chen CW, Jung HS, Jiang TX, Chuong CM. Asymmetric expression of Notch/Delta/Serrate is associated with the anterior-posterior axis of feather buds. Dev Biol. 1997; 188:181–187. [PubMed: 9245521]
50. Tumbar T, et al. Defining the epithelial stem cell niche in skin. Science. 2004; 303:359–363. [PubMed: 14671312]

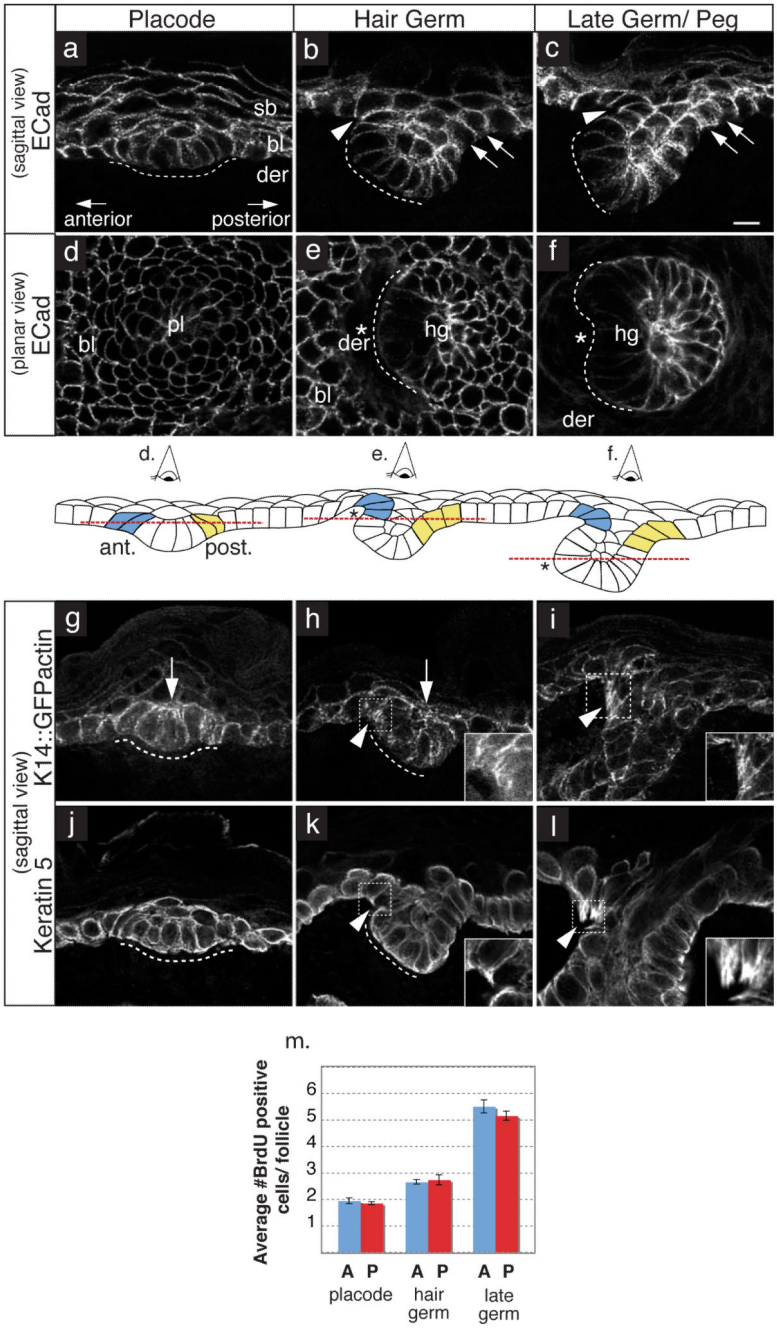

Figure 1. HF angling is accompanied by polarized cell shape and cytoskeleton changes in anterior and posterior cells at the HF-epidermal boundary

(**a–c**) Sagittal sections through E16.5 HFs labelled with E-Cadherin to mark cell-cell borders. (**a**) Hair placodes (dashed line) are symmetric when they first invaginate into the dermis. (**b–c**) In early and late hair germs, anterior follicle cells next to the epidermis constrict basally (arrowheads) while posterior cells do not (arrows). (**d–f**) Confocal sections of E15.5 whole mount epidermis labelled with E-Cadherin. By the early hair germ stage anterior cells (expressing reduced levels of ECad) adopt shapes/orientations distinct from

posterior cells. Asterisk denotes dermis (see schematic). Red dotted lines in schematic denote planes of view for images shown in (d-f). (**g–i**) Sagittal sections from E16.5 transgenic embryos expressing K14-GFPActin15. GFPActin is enriched in apical (arrows) and basal (arrowheads) constrictions. (**j–l**) Protrusions enriched for keratin 5 (K5) emanate from basal epidermal cells on the anterior but not posterior side of hair germs and E18.5 hair pegs. bl= basal layer; sb=suprabasal layers; der= dermis; pl= placode; hg= hair germ. Scale bar 10um. (**m**) Proliferation in developing HFs. BrdU was administered to E16.5 embryos and chased for 1 hour. Bars represent the average number of BrdU positive cells/ anterior or posterior side of HF. Total #HFs counted: 152 placodes, 147 early hair germs, 122 late hair germs. n=4 embryos.

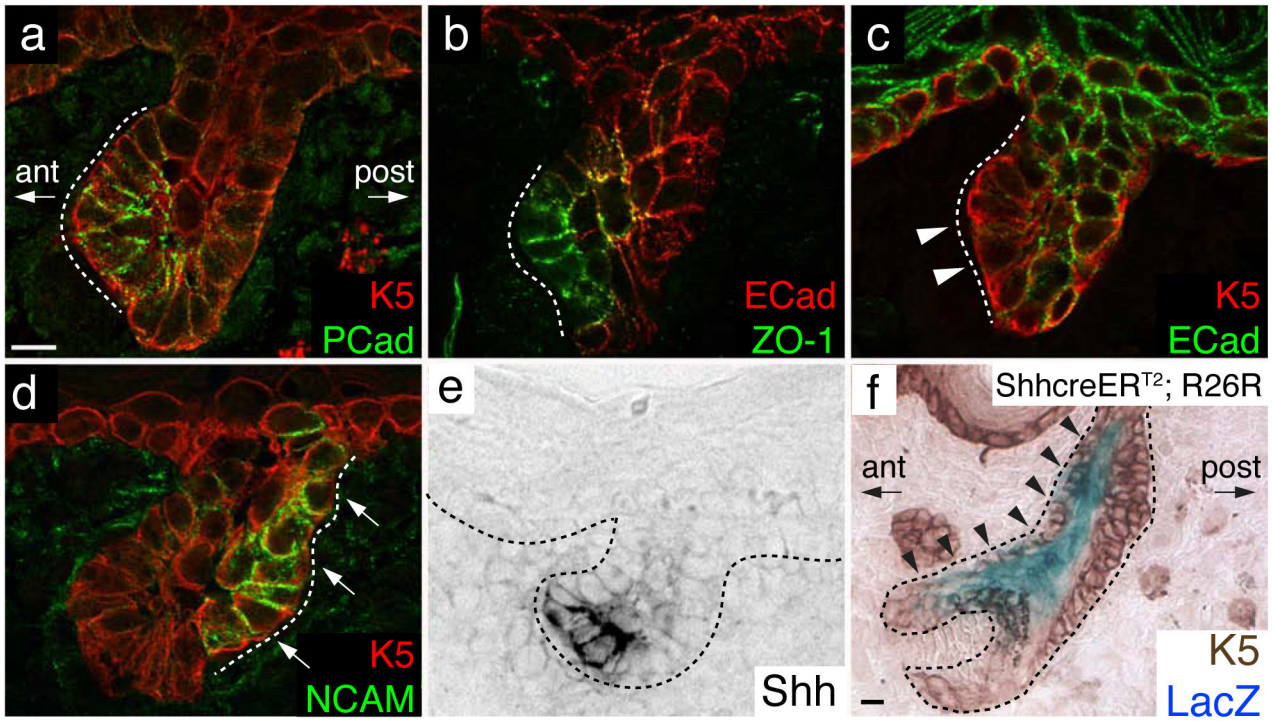

Figure 2. A-P-polarized gene expression in embryonic HFs

(**a–d**) Immunofluorescence images of E17.5 hair germs. Antibodies (Abs) colour coded according to the secondary Abs used. White dotted lines denote polarized zones for gene expression. Note upregulation of the adherens junction (AJ) protein P-cadherin (Pcad) and tight junction protein ZO-1 and downregulation of the AJ protein E-cadherin (Ecad) on the anterior side of cells in the lower portion of hair germs (arrowheads). Note upregulation of neural cell adhesion molecule (NCAM) on the posterior side of cells in the upper portion of the follicle (arrows). (**e**) Expression of the gene encoding signalling morphogen Shh by *in situ* hybridization. (**f**) Tracking early progeny of Shh-expressing cells through lineage tracing. *ShhCreER^{T2}; R26R* mice were treated with tamoxifen at E15.5. In P0 follicles LacZ-positive cells (blue, X-Gal staining) were only detected in the anterior and central portion of developing HFs. K5, keratin 5. Scale bars 10um.

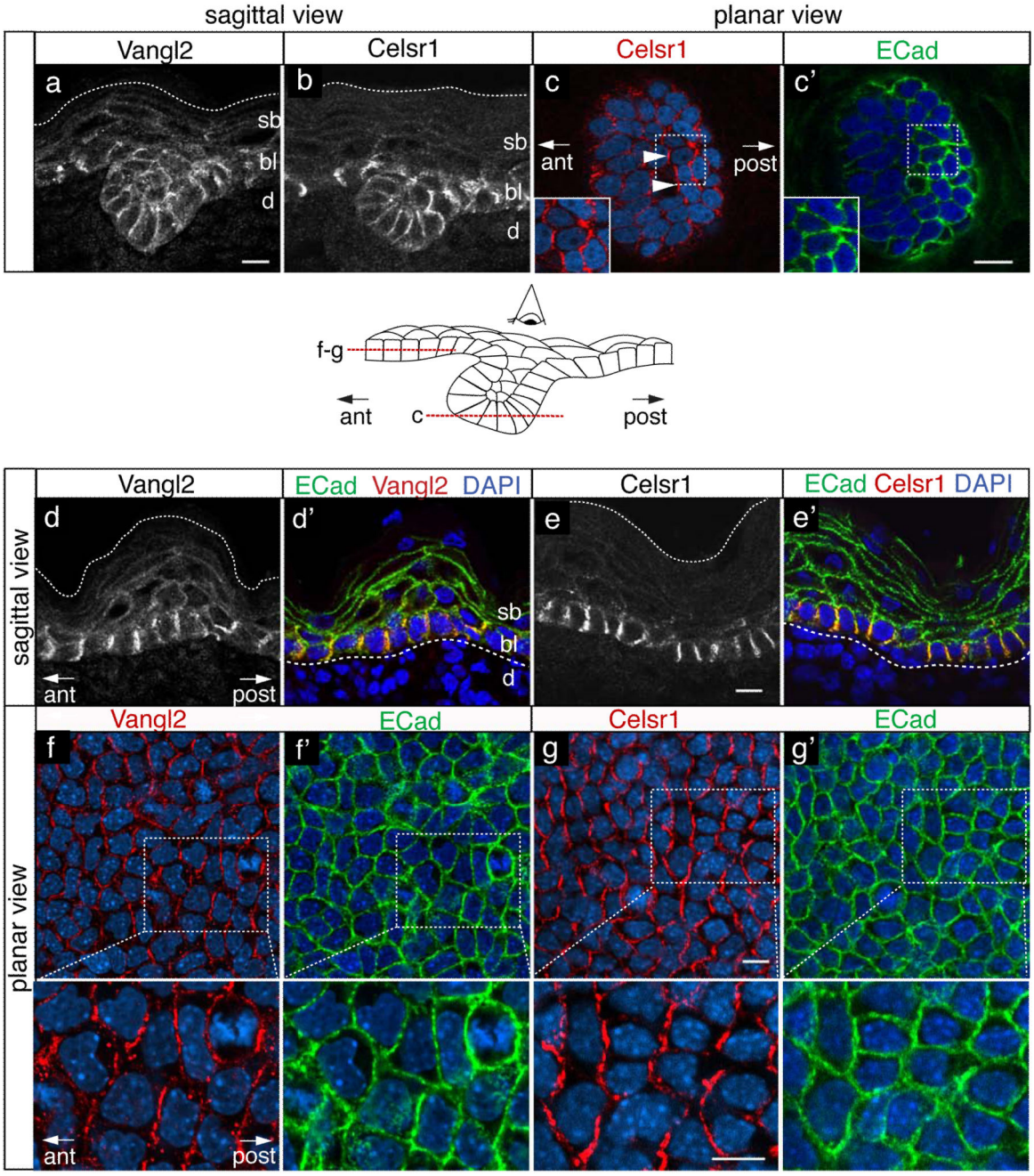

Figure 3. Anterior-Posterior polarization of Vangl2 and Celsr1 in the hair germs and the epidermal basal layer of embryonic skin

Schematic indicates each of the planar views in optical confocal sections of E15.5 whole mount skins. Abs are indicated overhead. Nuclei are labelled with DAPI (blue) except in (c-c') where transgenic expression of *K14*-H2B-GFP is pseudocoloured in blue. White dotted lines denote skin surface. Boxed areas are magnified as insets. (**a–c**) Expression and localization of Vangl2 and Celsr1 in hair germs. Note that Vangl2 and Celsr1 are polarized in the anterior-posterior lateral membranes of follicle cells, while E-cadherin is not. (**d–g**)

Expression and localization of Vangl2 and Celsr1 within the basal layer of embryonic epidermis. Again, while E-cadherin is uniformly distributed at cell-cell borders, Celsr1 and Vangl2 are polarized along the A–P axis. sb=suprabasal layers; bl= basal layer; d= dermis; hg= hair germ. Scale bars 10um.

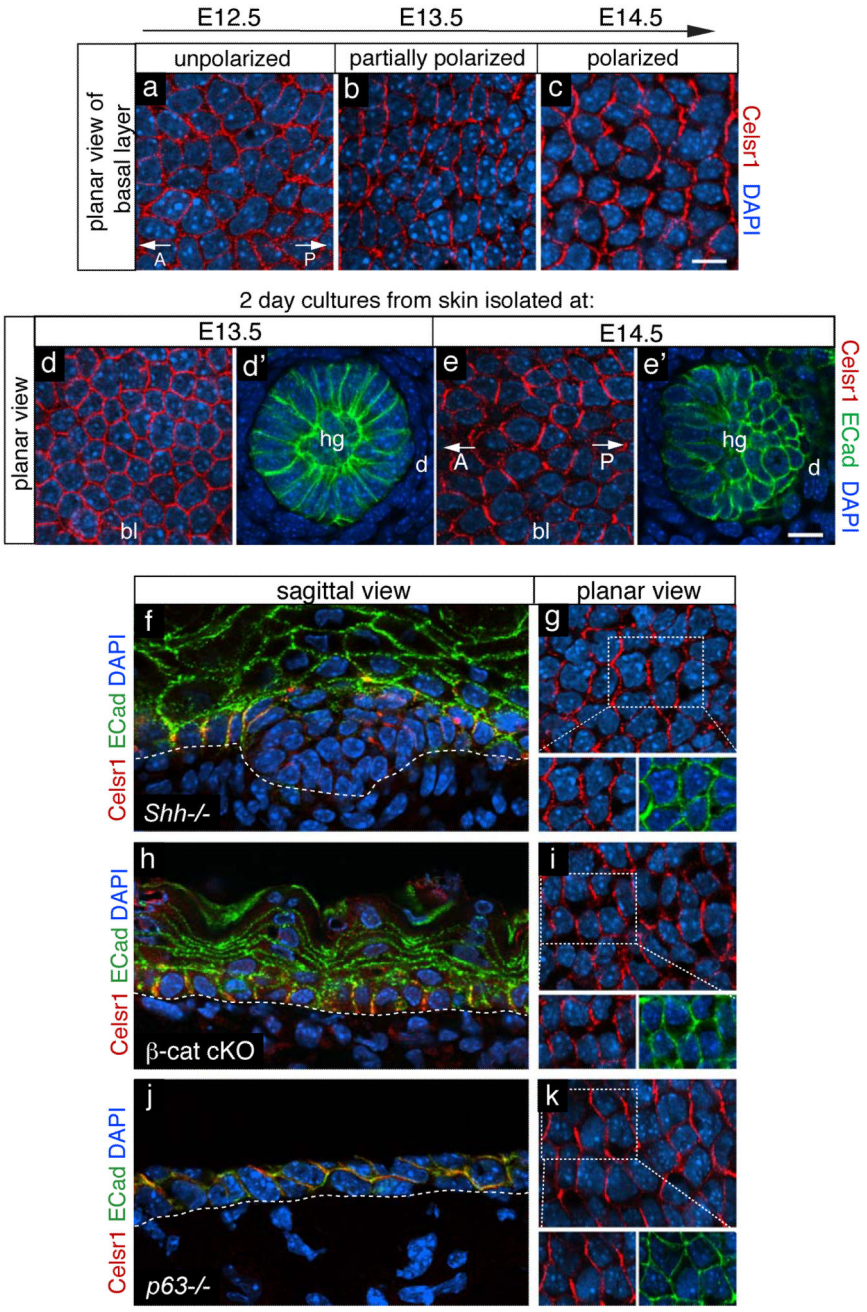

Figure 4. PCP establishment occurs early and requires signals from the embryo but develops independently of stratification and HF morphogenesis

(**a–c**) Confocal planar sections through the basal layer of whole mount E12.5–E14.5 skin labelled with Celsr1 antibodies and DAPI as indicated. Note that PCP begins to develop between E12.5 and E13.5, and is established by E14.5. (**d–e**) Skins were removed from E13.5 and E14.5 embryos and cultured *ex vivo* for two days under conditions permissive for HF morphogenesis. Afterwards, explants were labelled with Celsr1 (red), E-cadherin (green) and DAPI (blue) and imaged through the plane of the epidermis (d, e) or HF (d',e'). Note

that at E14.5 but not E13.5, epidermal PCP was maintained *in vitro* and nascent HFs still grew towards the anterior. (**f–k**) Sagittal and planar views of skins from embryos mutant for Shh, β-catenin or p63, labelled with Celsr1, E-cadherin and DAPI as indicated. Boxed areas are magnified, and co-labelling is shown to highlight that Celsr1 polarization in the basal layer is established independently of these early developmental regulatory pathways. hg= hair germ; d=dermis. Scale bars 10μm.

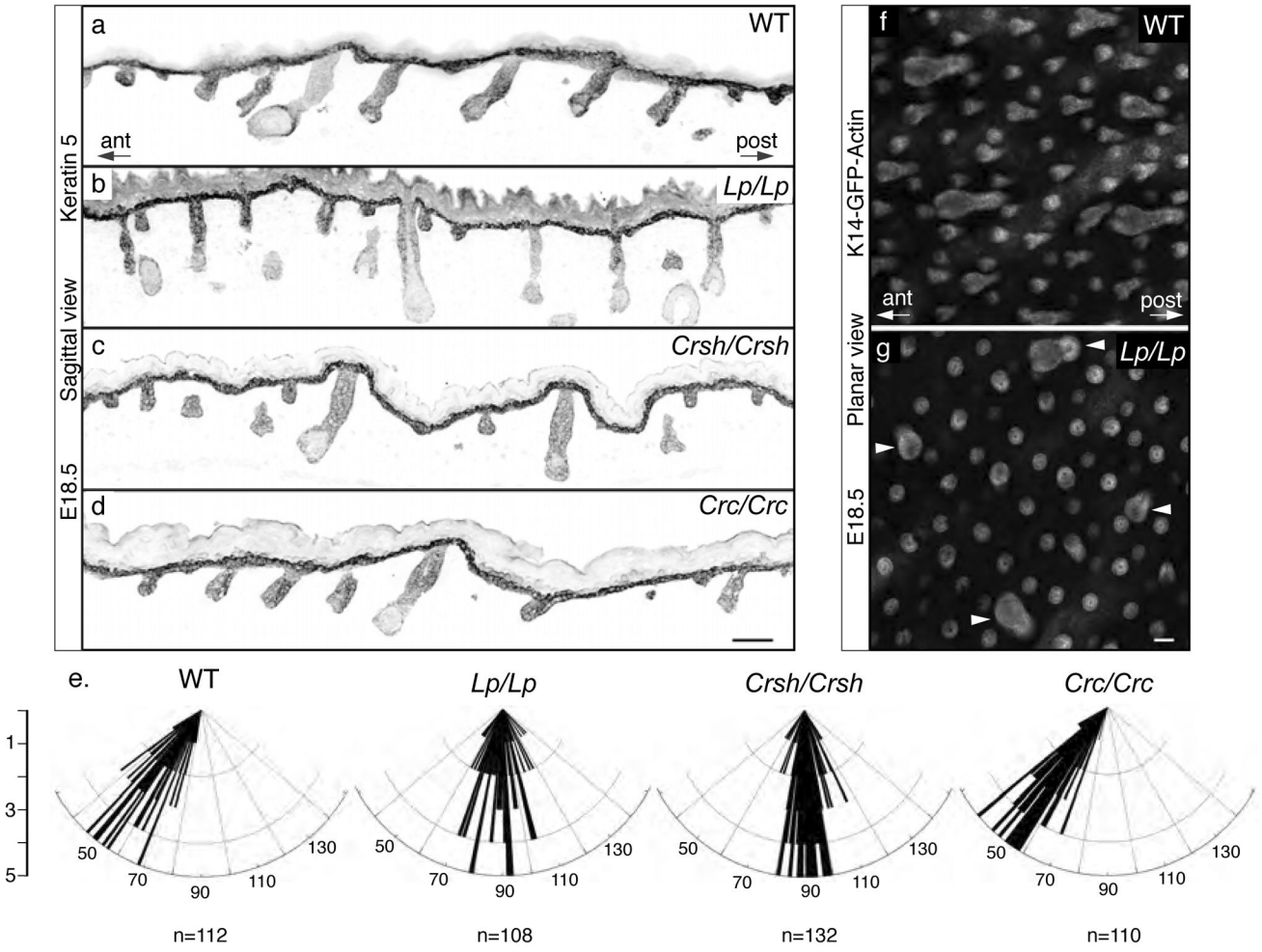

Figure 5. Genetic mutations in *Vangl2* and *Celsr1* result in loss of A–P alignment of hair follicles

(**a–d**) Saggital images of skin sections from WT, *Lp/Lp*, *Crsh/Crsh*, and *Crc/Crc* E18.5 embryos labelled with Abs against K5 and imaged at 10X magnification. (**e**) Schematics summarizing the quantifications of HF angles.×axis= angle between epidermis and HF on the anterior side. y-axis= number of follicles at angle x. The angles of ~10% of mutant follicles were oriented out of the plane of sectioning and hence were not measured. Note that *Crsh* (Celsr1) and *Lp* (Vangl2) mutants are defective in HF alignment, but *Crc* (Scribble), involved in some types of PCP, is not6. (**f–g**) Projected Z-stacks of whole mount epidermis from *Lp/+* and *Lp/Lp* embryos expressing K14-GFPactin at E18.5. Magnification 10X. Note that larger, more mature *Lp/Lp* follicles (arrowheads) orient randomly while early stage follicles (rest) point straight downward and appear uniformly circular by planar view. Scale bars 50μm.

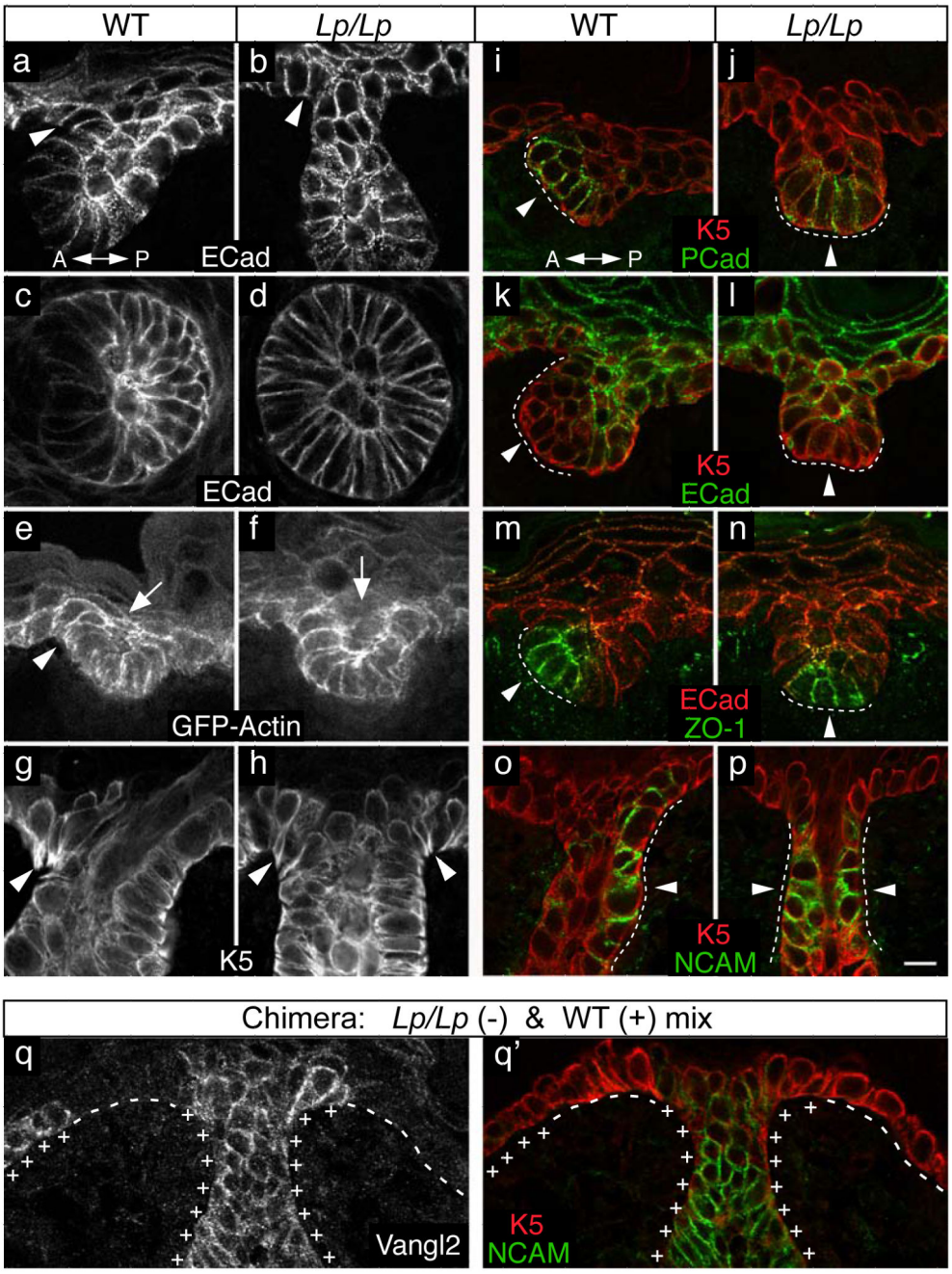

Figure 6. Loss of hair follicle asymmetry in PCP mutants

(**a–p**). Immunofluorescence microscopy of planar (c,d) or sagittal (rest) confocal skin sections from WT or *Lp/Lp* mutant embryos labelled with Abs or epifluorescence as indicated. (**a–b**) Anterior cells near the top of *Lp/Lp* follicles (E16.5) no longer constrict basally (arrowheads). (**c–d**) Loss of anterior-posterior asymmetry in architecture of *Lp/Lp* hair germs (E15.5). (**e–f**) E16.5 WT and *Lp/Lp* embryos on transgenic background of *K14-GFPactin*. Note that the apical enrichment (arrows) and basal constrictions (arrowheads) of F-actin are lost at the anterior-posterior junctions between *Lp/Lp* hair germs and epidermis.

(**g–h**) The asymmetric distribution of keratin 5 (K5) positive protrusions, typically on the anterior side of WT hair pegs at E18.5, is replaced by smaller K5-positive protrusions on both sides of *Lp* mutant hair pegs (arrowheads). (**i–p**) Intercellular adhesion proteins are no longer asymmetrically distributed within the anterior and posterior sides of hair germs in E17.5 *Lp/Lp* embryos. (**q–q'**) Chimeric embryos (E16.5) were generated from blastocysts composed of WT and *Lp/Lp* cells (see Experimental Procedures). WT cells are indicated by (+) symbols and are marked by the presence of Vangl2; *Lp/Lp* mutant cells are denoted by (−) symbols and marked by the absence of cell border Vangl2 staining (q). Note that despite consisting almost entirely of WT cells, HFs from chimeric mice fail to asymmetrically express NCAM (**q'**; green), or point towards the anterior when surrounded by *Lp/Lp* mutant interfollicular epidermal cells. Scale bars 10μm.

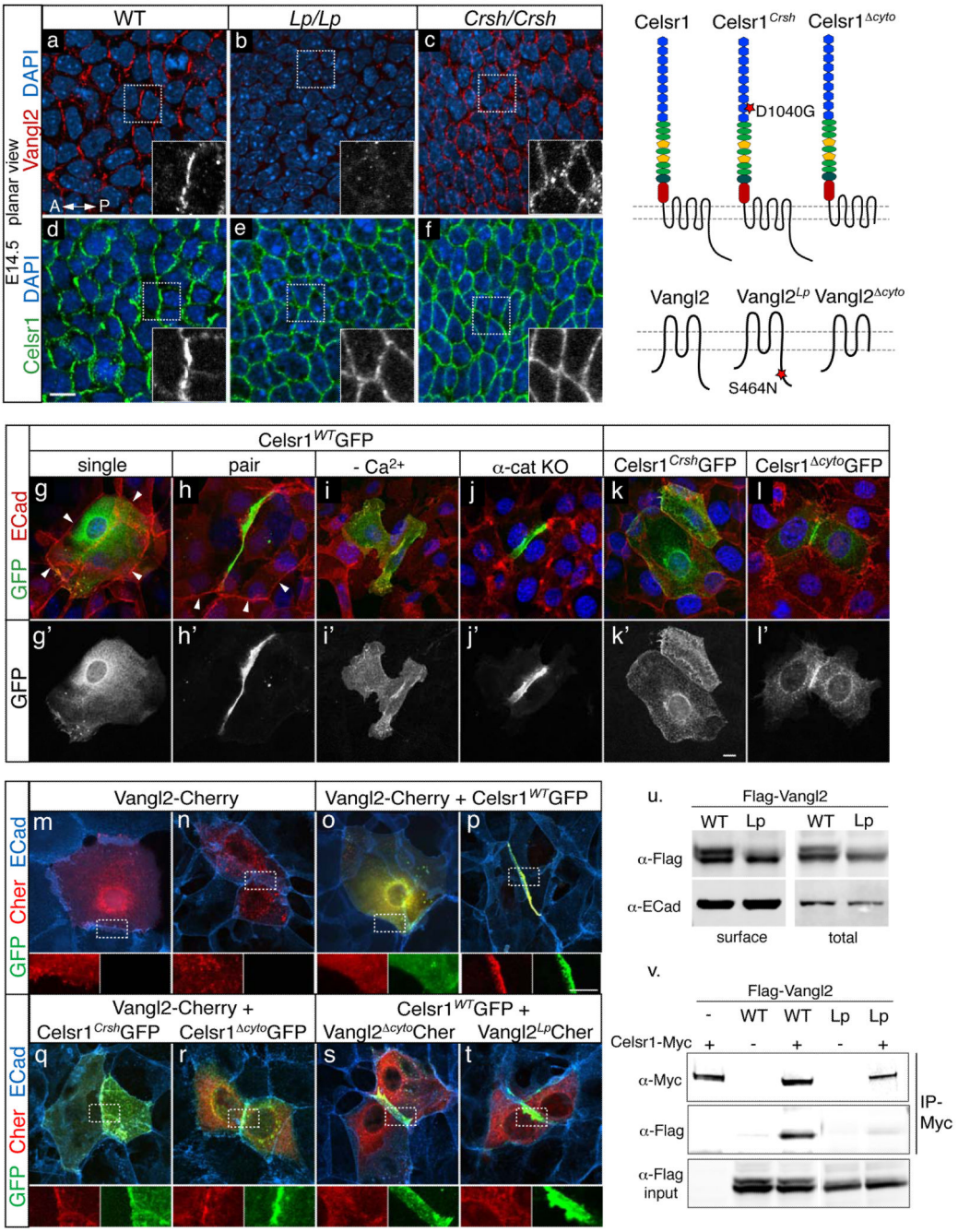

Figure 7. Evidence for interactions between Celsr1 and Vangl2 in vivo and in vitro

(**a–f**) *In vivo* studies. Planar confocal sections through the basal layer of whole mount skin from E15.5 WT, *Lp/Lp*, and *Crsh/Crsh* embryos, labelled with Celsr1 (green), Vangl2 (red) and DAPI (blue). Note that in *Lp/Lp* mutants, Celsr1's A–P polarity is lost. In *Crsh/Crsh* mutants both Celsr1 and Vangl2 lose A–P polarity, and Vangl2 is punctate and discontinuous at cell borders. Boxed areas are magnified in insets. (**g–t**) *In vitro* studies. Cultured keratinocytes expressing fluorescently tagged Celsr1, Vangl2 or their mutant versions as indicated. Confluent monolayers were shifted to high Ca^{2+} medium to induce the

formation of intercellular junctions, except in (**i**) where cells were kept in low Ca^{+2}. Each image shown is representative of ≥ 50 examples. Boxed areas are magnified, and red and green fluorescence is separated for additional clarity. Scale bars 10μm. Schematics depict domain structure of WT and mutant proteins. (**g–l**) Celsr1 data. Note that Celsr1^{WT}GFP shifts its localization to cell-cell borders in a calcium-dependent but α-catenin (adherens junction) independent fashion when two transfected cells come into direct contact. Note also that the Celsr1^{Crsh} mutant and Celsr1 lacking the C-terminal cytoplasmic tail (Δ*cyto*) are compromised in this ability. (**m–t**) Vangl2 and co-expression data. Note that Vangl2 is unable to localize to cell-cell borders on its own. In the presence of Celsr1^{WT}GFP, Cherry-Vangl2 shifts its localization to cell-cell borders only when two Celsr1-expressing cells are in direct contact (p), and mutant versions of Celsr1 are compromised in this ability (q–r). Cherry-Vangl2 mutants lacking the C-terminal cytoplasmic tail or carrying the *Lp* point mutation fail to be recruited by Celsr1 to cell contacts. (**u**) Surface biotinylation assay. Biotinylated surface proteins from keratinocytes expressing Flag-Vangl2^{WT} or Flag-Vangl2^{Lp} were recovered with streptavidin-coated sepharose beads and analyzed by Western blot to show that the *Lp* Vangl2 mutation does not appear to compromise the relative stability and/or cell surface localization of Vangl2. (**v**) Protein extracts from keratinocytes expressing Flag-Vangl2 ± Celsr1-Myc as indicated were immunoprecipitated with anti-Myc Abs. Flag-Vangl2^{WT} but not Flag-Vangl2^{Lp} coimmunoprecipitated with Celsr1-Myc.

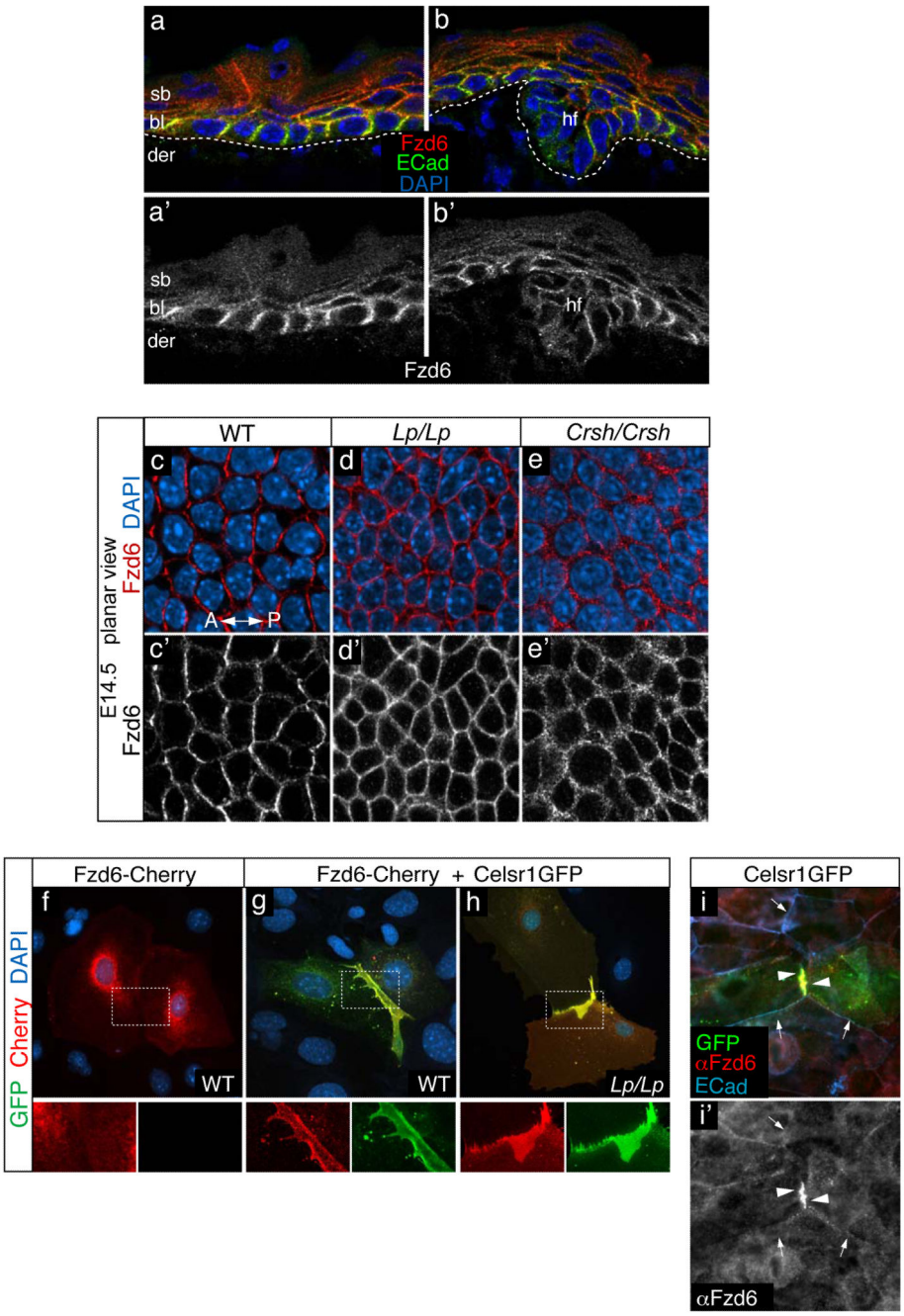

Figure 8. Fzd6 requires Vangl2 for its asymmetric localization in the epidermis and requires Celsr1 for it recruitment to cell contacts

(**a–b'**). Sagittal sections of WT E16.5 epidermis labelled with Abs as indicated. Like Celsr1 and Vangl2, Fzd6 is expressed in the basal layer (**a**) and early HFs (**b**), and is localized to lateral cell-cell borders. (**c–e**) Planar localization of Fzd6. Confocal sections through the basal layer of whole mount epidermis from WT, *Lp/Lp*, and *Crsh/Crsh* E15.5 embryos, labelled with Abs as indicated. Note enrichment of Fzd6 at A–P cell borders in WT, but not *Lp/Lp* and *Crsh/Crsh* epidermis. (**f–h**) Expression of Fzd6-Cherry and Celsr1-GFP in

keratinocyte monolayers. Note that in the presence of Celsr1-GFP, Cherry-Fzd6 is recruited to cell-cell borders only when two Celsr1 expressing cells are in direct contact. Fzd6 recruitment by Celsr1 also occurs normally in *Lp/Lp* mutant keratinocytes, suggesting that Vangl2 is not required for Fzd6 cell contact localization. (**i**) Endogenous Fzd6 localization in keratinocyte monolayers. In the absence of Celsr1-GFP, Fzd6 is distributed throughout the cell (arrows), but is recruited to the interface between two Celsr1-expressing cells (arrowheads).